# How to Dress Radio-Frequency Photons with Tunable Momentum

Boris Shteynas,[1,‡] Jeongwon Lee,[1,*,‡] Furkan Çağrı Top,[1] Jun-Ru Li,[1,†] Alan O. Jamison,[1]
Gediminas Juzeliūnas,[2] and Wolfgang Ketterle[1]
[1]Research Laboratory of Electronics, MIT-Harvard Center for Ultracold Atoms, Department of Physics, Massachusetts Institute of Technology, Cambridge, Massachusetts 02139, USA
[2]Institute of Theoretical Physics and Astronomy, Vilnius University, Saulėtekio 3, Vilnius 10257, Lithuania

(Received 18 July 2018; published 16 July 2019)

We demonstrate how the combination of oscillating magnetic forces and radio-frequency (rf) pulses endows rf photons with tunable momentum. We observe velocity-selective spin-flip transitions and the associated Doppler shift. Recoil-dressed photons are a promising tool for measurements and quantum simulations, including the realization of gauge potentials and spin-orbit coupling schemes which do not involve optical transitions.

DOI: 10.1103/PhysRevLett.123.033203

The field of cooling and trapping atoms depends on mechanical forces exerted by light through photon recoil [1]. Since photons can be scattered only by admixing electronically excited states, the mechanical forces due to light always involve dissipation by spontaneous emission. This is desirable in laser cooling but causes heating and atom loss in other situations where it is often suppressed by using far off resonant light (e.g., in optical lattices).

In this work we show how to dress radio-frequency (rf) photons with tunable recoil momentum by combining rf pulses with an oscillating magnetic force. This is a new application of Floquet engineering: periodically driven systems can have time-averaged properties which cannot be achieved with constant fields. Well-known examples are the Kapitza pendulum, Paul traps for ions, and the realization of Hamiltonians with complex tunneling matrix elements for ultracold atoms in optical lattices [2–4].

The question of how to replace photon recoil by other forces was raised in the context of spin-orbit coupling for ultracold atoms [5]. The well-established two-photon scheme is limited by heating due to spontaneous emission of photons. This limitation has motivated the development of alternative schemes which use time-dependent magnetic fields [6–9] to realize spin-dependent synthetic gauge fields. Some of those schemes are fairly complex, and have motivated the following question: Is it possible to Floquet engineer a rf or microwave transition between two spin states in such a way that it shows all aspects of recoil momentum?

With this motivation, we propose and demonstrate the new concept of recoil-dressed rf photons. This scheme allows us to conduct Doppler-sensitive spectroscopy and velocimetry of molecules when suitable optical transitions are not available. It is a building block for quantum simulations and offers a new approach for spin-orbit coupling using time-dependent magnetic forces. In our scheme, we drive rf transitions between two different hyperfine states in the presence of an alternating magnetic field gradient. The time-averaged evolution is a rf transition where recoil momentum is transferred. The sign and magnitude of the momentum kick is adjustable via the magnetic fields, and we observe a recoil momentum for the dressed photon which is $6 \times 10^6$ higher than the (usually negligible) momentum of a bare rf photon around 8 MHz frequency.

Our scheme shows the power of Floquet engineering: we combine a rf transition, which has negligible momentum transfer, with a sinusoidally oscillating magnetic field gradient, which has no time-averaged momentum transfer, and the result is a rf photon with recoil, depending on how rf pulses are synchronized with the time-dependent magnetic field gradient.

Figure 1 shows the time sequence of our scheme, which consists of a sinusoidal spin-dependent force $f(t) = g_F \mu_B B_0' \sin[(2\pi/T)t + \phi_{\mathrm{rf}}]\sigma_z$, where $g_F$ is the Lande factor, $\mu_B$ is the Bohr magneton, and $B_0'$ is the magnitude of the magnetic gradient, and a synchronized sequence of short rf pulses at times $t = 0, T, 2T, \ldots$. The timing of the pulses with respect to the periodic force is described by the phase $\phi_{\mathrm{rf}}$ which determines the magnitude of the photon recoil. Each of the rf pulses couples spin-up and spin-down states with the same momentary (i.e., at the time of the rf pulse) velocity $v_{\mathrm{rf}}$. For $\phi_{\mathrm{rf}} = 0$, the velocities averaged over a full cycle of the oscillating force, $\langle v_\uparrow \rangle$ and $\langle v_\downarrow \rangle$, are different. By flipping the spin, atoms experience an "extra" half-cycle of the magnetic acceleration [hatched area in Fig. 1(a)], which transfers them to the state with a different averaged velocity, and, therefore, provides recoil. For the case $\phi_{\mathrm{rf}} = \pi/2$, the time-averaged velocities for spin-up and spin-down are identical to $v_{\mathrm{rf}}$. Therefore, a rf transition will not change the time-averaged velocities, and there is no recoil.

 

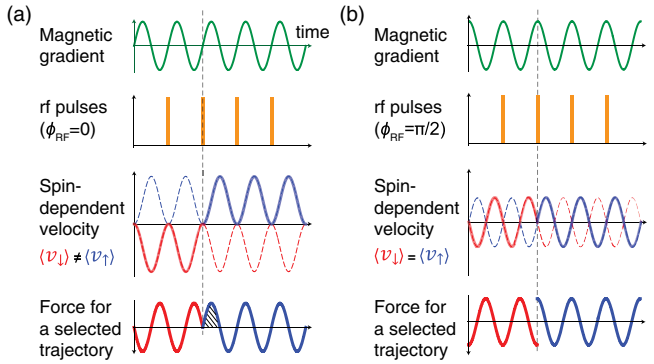


FIG. 1. Illustration of our scheme for creating a tunable atomic recoil momentum with rf transitions using magnetic forces. Panels (a) and (b) show the experimental conditions for $\phi_{\rm rf} = 0$ and $\phi_{\rm rf} = \pi/2$, respectively. The spin-dependent forces and velocities are shown (as thick solid lines) for the amplitude of the wave function which is transferred from spin-down (red) to -up (blue) by the rf pulse marked by the gray dashed line. For $\phi_{\rm rf} = 0$, the average velocities $\langle v_\downarrow\rangle$ and $\langle v_\uparrow\rangle$ are different, which implies a finite recoil associated with the spin flip. In contrast, $\langle v_\downarrow\rangle = \langle v_\uparrow\rangle$ for $\phi_{\rm rf} = \pi/2$, and there is no recoil.

Using this semiclassical picture, we obtain for the amount of momentum transfer $\hbar k = m(\langle v_\uparrow\rangle - \langle v_\downarrow\rangle) = \hbar k_0 \cos\phi_{\rm rf}$, where $k_0 = (g_F\mu_B/\pi\hbar)B_0' T$. Next we discuss where the change in kinetic energy comes from. For an optical transition with recoil $\hbar k$ and an atom moving at initial velocity $v_{\rm in}$, the resonance frequency is shifted by the Doppler shift $kv_{\rm in}$ and recoil shift $(\hbar k)^2/2m$, which ensures energy conservation. However, in the current situation, energy can also come from the time-dependent magnetic force. Indeed, if we would apply a single rf $\pi$ pulse at phase $\phi_{\rm rf} = 0$, the time-averaged velocity would change by $\hbar k_0/m$, but the rf resonance frequency would be independent of velocity and $k_0$. However, if a series of rf pulses is used, as in (Fig. 1), the resonance is Doppler shifted and becomes velocity selective. This can be seen by regarding the pulses as Ramsey pulses and considering the phase evolution of the wave function between two pulses. The rf pulses create a superposition of spin-up and spin-down. Between pulses, the phase evolution for spin-up or -down is solely determined by the kinetic energy $\alpha_{\uparrow\downarrow} = (1/\hbar)\int(mv_{\uparrow\downarrow}^2/2)dt$, leading to a phase difference $\delta\alpha = (1/\hbar)(m(\langle v_\uparrow\rangle - \langle v_\downarrow\rangle)v_{\rm rf})T = kv_{\rm rf}T$ after one period of shaking, where $v_{\rm rf} = (v_\uparrow + v_\downarrow)/2$ is the common velocity at the moment of the rf pulse. With $\langle v_\downarrow\rangle = v_{\rm rf} - \hbar k/2m$, we find that for resonant excitation, the rf has to compensate for this phase shift by the Doppler detuning $k\langle v_\downarrow\rangle$ and the recoil shift $(\hbar k)^2/2m$ (see Supplemental Material for more details [13]).

Periodic Hamiltonians are formally treated by Floquet theory [2,3,15–17], which provides an expression for an effective Hamiltonian $\hat{H}_{\rm eff}$ describing the slow time evolution of the system averaged over the fast micromotion with period $T$. However, in the standard treatment the effective Hamiltonian is not unique and may depend on the initial time when the periodic drive is switched on. We adopt the approach of Ref. [2], where the evolution of the quantum system with periodic drive is expressed by an effective Hamiltonian independent of initial and final times $t_i$, $t_f$ and a kick (micromotion) operator $\hat{K}$, which describes the initial kick due to a sudden switch on and the subsequent micromotion, shown as $\hat{U}(t_f, t_i) = e^{-i\hat{K}(t_f)}e^{-i\hat{H}_{\rm eff}(t_f - t_i)}e^{i\hat{K}(t_i)}$.

For our scheme, the time-dependent Hamiltonian of the system in the frame rotating with the rf drive after the rotating-wave approximation is

$$\hat{H} = \frac{\hat{p}_z^2}{2m} + \hbar k_0 \hat{z}\frac{\pi}{T}\sin(2\pi t/T + \phi_{\rm rf})\hat{\sigma}_z - \frac{1}{2}\hbar\delta_{\rm rf}\hat{\sigma}_z + \hbar\Omega\hat{\sigma}_x T\sum_n \delta(t - nT), \tag{1}$$

where $\delta_{\rm rf}$ is the rf detuning with respect to the atomic resonant frequency and $m$ is the atomic mass. The short rf pulses are represented as a series of delta functions with effective Rabi frequency $\Omega$.

Through the derivation shown in the Supplemental Material [13], we obtain an explicit expression for the effective Hamiltonian and the kick operator defined above:

$$\hat{H}_{\rm eff} = \begin{pmatrix} \frac{\hat{p}_z^2}{2m} + \frac{1}{16}\frac{\hbar^2 k_0^2}{m} - \frac{\hbar\delta_{\rm rf}}{2} & \hbar\Omega e^{-ik_0\cos\phi_{\rm rf} z} \\ \hbar\Omega e^{ik_0\cos\phi_{\rm rf} z} & \frac{\hat{p}_z^2}{2m} + \frac{1}{16}\frac{\hbar^2 k_0^2}{m} + \frac{\hbar\delta_{\rm rf}}{2} \end{pmatrix},$$
$$\hat{K}(t) = -ik_0 z\hat{\sigma}_z \cos\left(\frac{2\pi}{T}t + \phi_{\rm rf}\right). \tag{2}$$

The effective Hamiltonian is identical to the one for a two-level atom driven by a photon field at frequency $\omega_{\rm rf}$ and with wave vector $k$, which confirms our discussion above about recoil momentum and Doppler shift. The term $\hbar^2 k_0^2/16m$ is the kinetic energy due to micromotion.

We implemented this scheme using a thermal cloud of approximately $1 \times 10^5$ $^{23}$Na atoms at 380 nK in a crossed optical dipole trap with trapping frequencies $(\omega_x, \omega_y, \omega_z) = 2\pi(98, 94, 25)$ Hz corresponding to Gaussian radii of 19.5, 20, and 68 $\mu$m, respectively. The $|m_F = -1\rangle$ and $|m_F = 0\rangle$ states of the $F = 1$ hyperfine manifold of the atoms were used to form a pseudospin-1/2 system, which will be referred to as $|\uparrow\rangle$ and $|\downarrow\rangle$ states, respectively. The $|m_F = 1\rangle$ state was decoupled from this two-level system through the quadratic Zeeman effect at a bias field of 11.4 G. Since there is no micromotion in the "nonmagnetic" $|m_F = 0\rangle$ state, the maximum momentum transfer $\hbar k_0$ is reduced by a factor of 2 compared to the discussion above.

The oscillating magnetic force was created by a time-dependent 3D quadrupole field. Along the bias field direction $z$, this provides a 1D periodic force. Orthogonal to the bias field, the periodic potential is quadratic—there is no net force, only a (negligible) modulation of the confinement.

The amplitude of the magnetic field gradient was 48 G/cm at a frequency of 5 kHz, implying a recoil $k_0 = 0.07k_L$, where $\hbar k_L$ is the recoil of the resonant transition at 589 nm, with a recoil velocity $(\hbar k_L/m) = 2.9$ cm/s.

To resolve Doppler shifts of 200 Hz, sub-mG stability was needed. Any asymmetry of the periodic magnetic field gradient leads to a time-averaged dc field gradient resulting in an inhomogeneous Zeeman shift which had to be suppressed at the 100 Hz level. Finally, the applied magnetic fields were modified by eddy currents in the stainless steel chamber, which had to be accounted for (see Supplemental Material [13]).

The goal of the experimental demonstration was to show that the rf transition is now Doppler sensitive due to the recoil transfer. The spin-flip transitions were driven by 4 $\mu$s long rf pulses at 8 MHz with a Rabi frequency of 10 kHz resulting in approximately $\pi/12$ pulses and an average Rabi frequency of $\Omega = 200$ Hz, which is defined as the Rabi frequency of the pulse times the duty cycle. Since it was not possible to switch off the shaking coils on microsecond timescales, the rf pulses had to be applied with the magnetic shaking present, which required several steps of spatial and temporal alignments (see Supplemental Material [13]).

The rf pulses and the shaking were applied while the atoms were trapped to ensure that the velocity distribution is independent of position. In time of flight (TOF), this is no longer the case, and any residual Zeeman shift gradients could lead to velocity selection. To avoid broadening of the Doppler selected velocity groups by the trapping potential, the total interrogation was chosen to be 1.6 ms, much shorter than the trap period along the $z$ direction. This time is also comparable to the coherence time due to the ambient magnetic field stability. Based on these considerations, we applied a pulse sequence of 2 ms consisting of 10 magnetic shaking cycles with 9 rf pulses across them.

The temperature of the cloud was chosen to be high enough that the Doppler width of 3 kHz (FWHM) was larger than our spectral resolution, mainly Fourier limited to 625 Hz by the 1.6 ms pulse sequence. Because of the Doppler shift, different detunings of the rf selected different velocity groups which were observed in ballistic expansion (Fig. 2). The width of the observed spin-flipped slices is almost completely determined by the original spatial size of the cloud since the expansion time of $\tau = 12$ ms was only twice the inverse of $\omega_z$. The TOF was limited by the signal-to-noise ratio, given the constraints discussed above. Fortunately, even for small TOF, the displacement of the center of the spin-flipped atoms is exactly $v\tau$, which could be accurately measured as a function of rf detuning, as shown in Fig. 3. The observed Doppler shift is in agreement with the theoretical treatment above and confirms that rf photons have been Floquet engineered to have recoil of $k = 0.07k_L$.

The dependence of the recoil on the rf phase was demonstrated by shifting the rf phase from 0 to $\pi$ [Fig. 3(b)]. The Doppler shift and therefore the direction

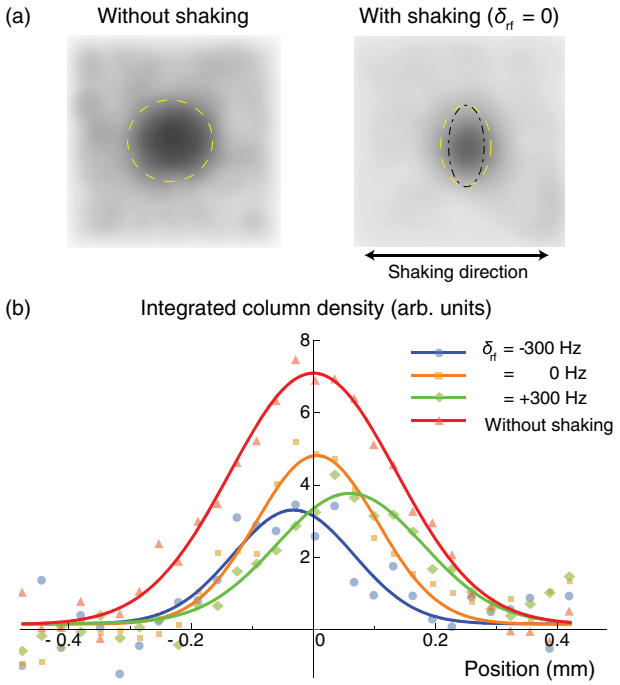


FIG. 2. Observation of velocity-selective rf transitions. (a) Absorption images of the spin-flipped atoms (i.e., in the $|m_F = -1\rangle$ state) after 12 ms of TOF with and without magnetic shaking. The yellow dashed ellipses have major and minor axes obtained as FWHM of Gaussian fits. After TOF, the thermal could expand by a factor of 2.13; thus, a single-velocity class is narrower than the thermal cloud by $1/2.13 \approx 0.47$. The Fourier limit of our velocity selection increases this to 0.50, and inclusion of eddy currents further modifies it to 0.45 (dash-dotted line). The field of view is $1 \times 1$ mm$^2$. (b) Integrated column density distribution obtained from absorption images like those in (a), for different rf detunings. The solid lines are Gaussian fits to the data points. The rf phase was at $\phi_{rf} = 0$ to maximize Doppler sensitivity. The asymmetry between the $\pm 300$ Hz is most likely caused by bias field drifts (estimated in Fig. 3 to be 70 Hz) or small residual magnetic field gradients.

of the recoil changed sign. This observation confirmed that the selection of slices in Fig. 2 is not due to time-averaged magnetic field gradients, which do not depend on the rf phase. We could not experimentally explore $\phi_{rf} = \pi/2$, since this would have required to pulse on the rf at the maximum field gradient, which would have caused large spatially dependent detunings.

Our scheme can be used to implement one-dimensional spin-orbit coupling of ultracold atoms with magnetic forces and without lasers. The Hamiltonian [Eq. (3)] which we have implemented is, by a unitary transformation, equivalent to a Hamiltonian with spin-dependent gauge fields [4]:

$$\hat{H}_{\mathrm{SOC}} = \frac{1}{2m}\left(\hat{p}_z - \frac{1}{2}A\hat{\sigma}_z\right)^2 + \hbar\Omega\hat{\sigma}_x - \frac{\hbar\delta_{\mathrm{rf}}}{2}\hat{\sigma}_z. \quad (3)$$

We note that Ref. [14] obtains the same Hamiltonian as the stroboscopic Floquet Hamiltonian. The gauge field

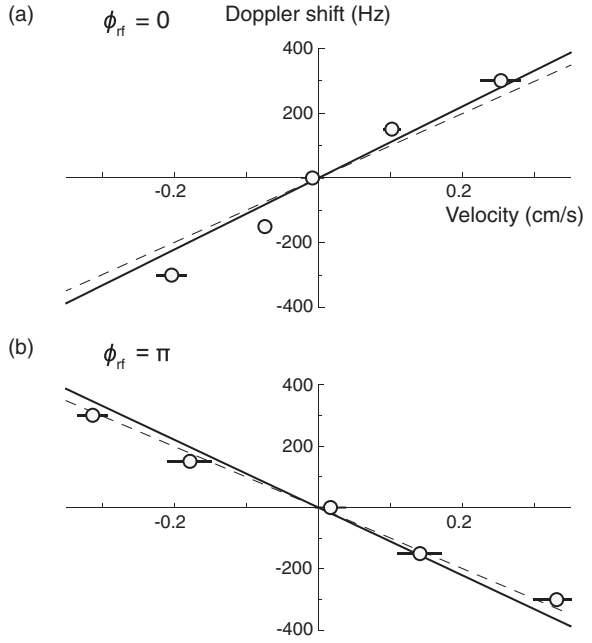


FIG. 3. Observation of rf transitions with Doppler shifts. (a), (b) Central velocities of the spin-flipped atomic distribution [as in Fig. 2(b)] are shown as a function of rf detuning for $\phi_{\mathrm{rf}} = 0$ and $\phi_{\mathrm{rf}} = \pi$, respectively. Shifting the rf phase changes the sign of the Doppler shift and therefore the direction of the recoil momentum. The solid line represents the predicted Doppler shifts based on the calibration of recoil momentum. The dashed line takes into account the effects of eddy currents (see Supplemental Material [13]). The error bars are purely statistical based on five data points and correspond to 1 standard deviation. The inferred $1\sigma$ fluctuations for the frequency are 70 Hz.

$A = \hbar k_0 \cos\phi_{\mathrm{rf}}$ is equal to the recoil momentum transfer $\hbar k$, which depends on the rf phase $\phi_{\mathrm{rf}}$. Previous experimental studies claimed the realization of spin-orbit coupling and gauge fields purely by magnetic shaking, without rf transitions [8,18]. These claims are ambiguous based on our discussion here: without rf coupling, the momentum transfer and the gauge field are not defined and can be transformed away with a gauge transformation. According to Eqs. (1) and (3), pure magnetic shaking leads only to a kick operator for the micromotion, and the effective Hamiltonian is the free-particle Hamiltonian. Therefore, all observations in Refs. [8,18] are related to an initial kick and micromotion and not to a modified effective Hamiltonian.

In the presence of gauge fields, there are two momenta: the mechanical or kinetic momentum $(p_z \pm \frac{1}{2}A)$ and the canonical momentum $p_z = mv_{\mathrm{rf}}$. In our scheme, they can both be directly observed and have a very transparent meaning: the kinetic momenta are the time-averaged momenta $m\langle v_\uparrow\rangle$, $m\langle v_\downarrow\rangle$. The canonical momentum is the instantaneous momentum during the rf pulse (see Supplemental Material [13]).

Our demonstration of rf dressed photons was done with a modest recoil $k_0$ of $0.07k_L$ due to technical limitations (see Supplemental Material [13]). The recoil could have been increased by using a glass cell, miniature coils, or atomic chips for which 12 times larger magnetic field gradients have been assumed [6]. Given the small value of $k_0$, we did not look for recoil effects in Bose-Einstein condensates, as in Ref. [19], and rather focused on Doppler shifts in thermal clouds.

Dressed-photon recoil has several features different from optical photon recoil: The maximum recoil of a dressed photon is only technically limited, and can be tuned via the strength of the magnetic gradient and in principle also via the rf phase, whereas the recoil in a two-photon transition can be tuned via the angle between the two laser beams. Heating for optical recoil transfer is independent of momentum transfer and depends on the Rabi frequency, whereas the reverse applies to the magnetic scheme.

As in any Floquet schemes, micromotion can lead to heating when the associated kinetic energy is transferred to the secular motion by elastic collisions between the two spin states (which is equivalent to transitions between Floquet states of different quasienergies). In Ref. [20], we describe various cases (high and low temperature limit, bosons, and fermions) and conclude that the energy transfer can be expressed by $\dot{E} \propto \rho\sigma v_{\mathrm{col}} E_0$, where $v_{\mathrm{col}}$ reflects an effective density of states. For Bose-Einstein condensates, $v_{\mathrm{col}} = \sqrt{\hbar\omega/m}$ for large modulation frequencies $\omega$, implemented in our experiments, and $v_{\mathrm{col}} = \hbar k_0/m$ in the semiclassical regime. Here, $\rho$ is the density and $\sigma$ is the two-body $s$-wave scattering cross section. For a sodium condensate with two spin components and density $\rho \sim 10^{14}$ cm$^{-3}$, we observed a condensate lifetime of $\sim$8 s at $k_0 = 0.05k_L$, consistent with weak Floquet heating [20]. If the momentum transfer $k_0$ is scaled up to $k_L$, losses increase proportional to the second or third power of $k_0$, depending on the regime [20]. For momentum transfers of $k_L$, lifetimes larger than 100 ms will require low density clouds on the order of $\sim 10^{12}$ cm$^{-3}$ or small scattering lengths. For degenerate Fermi gases with $E_{\mathrm{F}} \gg \hbar\omega$, heating is Pauli suppressed by a factor of $(\hbar\omega/E_F)^2$.

There are possible extensions of generating magnetic recoil. One is to use the time-averaged, orbiting potential (TOP) trap configuration [21], where a constant gradient is combined with a rotating bias field in the $x$-$y$ plane, which creates a rotating force. A sequence of rf pulses generates "dressed photons" with recoil $k$ along the $\cos\phi_{\mathrm{rf}}\mathbf{e}_x + \sin\phi_{\mathrm{rf}}\mathbf{e}_y$ direction. The rf phase now controls the direction of the recoil. The concept of dressed rf photons should be useful for a more general class of quantum simulations. For instance, it applies to spin-dependent forces created by the vector ac Stark shift. Using focused laser beams or lattices to create spin-dependent potentials, the effective recoil is spatially localized, and can easily be time modulated. In comparison to magnetic field gradients, the forces due to the vector ac Stark shift can be larger, and much faster modulation frequencies are possible. Using optical spin-dependent

forces instead of magnetic forces may eliminate several limitations of our scheme, especially for atoms like cesium and rubidium, where large spin-dependent optical forces can be realized without major heating by spontaneous scattering.

In conclusion, we demonstrated how magnetic shaking can be used to endow a rf photon with large and tunable recoil. This scheme illustrates many aspects of Floquet engineering, including heating in both the quantum and classical limit. This technique is a building block for quantum simulations including spin-dependent gauge fields and measurements such as Doppler velocimetry. It can be applied to any atom or molecule with nonzero spin in the ground state, and is independent of the structure of electronically excited states.

We would like to acknowledge Will Lunden for experimental assistance, Ivana Dimitrova for critical reading of the manuscript, and Viktor Novičenko for discussions. We acknowledge support from the NSF through the Center for Ultracold Atoms and Grant No. 1506369, from ARO-MURI Non-equilibrium Many-body Dynamics (Grant No. W911NF-14-1-0003), from AFOSR-MURI Quantum Phases of Matter (Grant No. FA9550-14-1-0035), from ONR (Grant No. N00014-17-1-2253), and a Vannevar-Bush Faculty Fellowship. Part of this work was performed at the Aspen Center for Physics, which is supported by NSF Grant No. PHY-1607611.

[*] jwlee0705@gmail.com
Present address: The Institute for Advanced Study, The Hong Kong University of Science and Technology, Clear Water Bay, Kowloon, Hong Kong.
[†] Present address: JILA, NIST and University of Colorado, 440 UCB, Boulder, Colorado 80309, USA.
[‡] B. S. and J. L. contributed equally to this work.

[1] C. Cohen-Tannoudji, J. Dupont-Roc, and G. Grynberg, *Atom-Photon Interactions: Basic Process and Applications* (Wiley, New York, 2008).
[2] N. Goldman and J. Dalibard, Phys. Rev. X **4**, 031027 (2014).
[3] M. Bukov, L. D'Alessio, and A. Polkovnikov, Adv. Phys. **64**, 139 (2015).
[4] J. Dalibard, F. Gerbier, G. Juzeliūnas, and P. Öhberg, Rev. Mod. Phys. **83**, 1523 (2011).
[5] V. Galitski and I. B. Spielman, Nature (London) **494**, 49 (2013).
[6] B. M. Anderson, I. B. Spielman, and G. Juzeliūnas, Phys. Rev. Lett. **111**, 125301 (2013).
[7] Z.-F. Xu, L. You, and M. Ueda, Phys. Rev. A **87**, 063634 (2013).
[8] X. Luo, L. Wu, J. Chen, Q. Guan, K. Gao, Z.-F. Xu, L. You, and R. Wang, Sci. Rep. **6**, 18983 (2016).
[9] For relevant work with modulated magnetic field in optical lattices, see Refs. [10–12].
[10] J. Struck, J. Simonet, and K. Sengstock, Phys. Rev. A **90**, 031601(R) (2014).
[11] G. Jotzu, M. Messer, F. Görg, D. Greif, R. Desbuquois, and T. Esslinger, Phys. Rev. Lett. **115**, 073002 (2015).
[12] J. Yu, Z.-F. Xu, R. Lü, and L. You, Phys. Rev. Lett. **116**, 143003 (2016).
[13] See Supplemental Material at http://link.aps.org/supplemental/10.1103/PhysRevLett.123.033203 for the derivation of the effective Hamiltonian, which includes Refs. [2,6,14].
[14] See Supplemental Material in X. Luo, L. Wu, J. Chen, Q. Guan, K. Gao, Z.-F. Xu, L. You, and R. Wang, Sci. Rep. **6**, 18983 (2016).
[15] A. Eckardt and E. Anisimovas, New J. Phys. **17**, 093039 (2015).
[16] V. Novičenko, E. Anisimovas, and G. Juzeliūnas, Phys. Rev. A **95**, 023615 (2017).
[17] A. Eckardt, Rev. Mod. Phys. **89**, 011004 (2017).
[18] L.-N. Wu, X.-Y. Luo, Z.-F. Xu, M. Ueda, R. Wang, and L. You, Sci. Rep. **7**, 46756 (2017).
[19] Y.-J. Lin, K. Jimenez-Garcia, and I. B. Spielman, Nature (London) **471**, 83 (2011).
[20] J.-R. Li, B. Shteynas, and W. Ketterle, arXiv:1906.08747.
[21] W. Petrich, M. H. Anderson, J. R. Ensher, and E. A. Cornell, Phys. Rev. Lett. **74**, 3352 (1995).